



HAL
open science

An interstellar origin for high-inclination Centaurs

Fathi Namouni, M. Morais

► **To cite this version:**

Fathi Namouni, M. Morais. An interstellar origin for high-inclination Centaurs. Monthly Notices of the Royal Astronomical Society, 2020, 494 (2), pp.2191-2199. 10.1093/mnras/staa712 . hal-02617138

HAL Id: hal-02617138

<https://hal.science/hal-02617138>

Submitted on 26 Aug 2022

HAL is a multi-disciplinary open access archive for the deposit and dissemination of scientific research documents, whether they are published or not. The documents may come from teaching and research institutions in France or abroad, or from public or private research centers.

L'archive ouverte pluridisciplinaire **HAL**, est destinée au dépôt et à la diffusion de documents scientifiques de niveau recherche, publiés ou non, émanant des établissements d'enseignement et de recherche français ou étrangers, des laboratoires publics ou privés.

An interstellar origin for high-inclination Centaurs

F. Namouni ¹★ and M. H. M. Morais ²★

¹Université Côte d'Azur, CNRS, Observatoire de la Côte d'Azur, CS 34229, F-06304 Nice, France

²Instituto de Geociências e Ciências Exatas, Universidade Estadual Paulista (UNESP), Av. 24-A, 1515, 13506-900 Rio Claro, SP, Brazil

Accepted 2020 March 7. Received 2020 March 6; in original form 2019 September 30

ABSTRACT

We investigate the possible origins of real high-inclination Centaurs and trans-neptunian objects using a high-resolution statistical search for stable orbits that simulates their evolution back in time to the epoch when planet formation ended 4.5 billion years in the past. The simulation is a precise orbit determination method that does not involve ad hoc initial conditions or assumptions such as those found in planetesimal disc relaxation models upon which their conclusions depend. It can therefore be used to independently test origin theories based on relaxation models by examining the past orbits of specific real objects. Here, we examined 17 multiple-opposition high-inclination Centaurs and the two polar trans-neptunian objects 2008 KV42 and (471325) 2011 KT19. The statistical distributions show that their orbits were nearly polar 4.5 Gyr in the past, and were located in the scattered disc and inner Oort cloud regions. Early polar inclinations cannot be accounted for by current Solar system formation theory as the early planetesimal system must have been nearly flat in order to explain the low-inclination asteroid and Kuiper belts. Furthermore, the early scattered disc and inner Oort cloud regions are believed to have been devoid of Solar system material as the planetesimal disc could not have extended far beyond Neptune's current orbit in order to halt the planet's outward migration. The nearly polar orbits of high-inclination Centaurs 4.5 Gyr in the past therefore indicate their probable early capture from the interstellar medium.

Key words: celestial mechanics – comets: general – Kuiper belt: general – minor planets, asteroids: general – Oort Cloud.

1 INTRODUCTION

Centaurs are some of the most intriguing objects in the Solar system. With perihelia and mean orbits inside the giant planets' domain, they are subjected to some of the strongest interactions in the Solar system. With moderate to high eccentricities, Centaurs' orbits may be inclined by a few degrees with respect to the Solar system's invariable plane to almost 180° resulting in retrograde motion. Their orbital features are often taken as a sign of their violent past in the Solar system, a notion reinforced by their so-called instability. If a Centaur orbit is integrated forward or backward in time, it will invariably either hit the Sun, the planets, or be ejected from the Solar system. As the gravitational dynamics of N -body systems is time-reversible, the values of the future and past lifetimes are statistically similar (Horner, Evans & Bailey 2004; Portegies Zwart & Boekholt 2018) and range from 1 to 100 Myr (Tiscareno & Malhotra 2003; Di Sisto & Brunini 2007; Bailey & Malhotra 2009; Volk & Malhotra 2013).

The exact meaning of this 'instability' is, however, unclear. The future lifetime is simple to interpret literally as the Centaurs are

simply ejected from the Solar system by their encounters with the planets or experience a planetary or solar collision. This should occur in the near future in view of the 1–100 Myr estimates of the future lifetime (Peixinho et al. 2020). The past lifetime is trickier to interpret literally because it would mean the Centaurs cannot have lived in the Solar system more than 1–100 Myr in the past. This indicates that they must all have been captured from the interstellar medium in the recent past.¹ Conventional models that study the origin of outer Solar system objects do not advocate this idea as they rely on the relaxation of the flat planetesimal disc present 4.6 Gyr in the past to explain not only Centaurs but all known outer Solar system bodies (Levison & Duncan 1997; Tiscareno & Malhotra 2003; Emel'yanenko, Asher & Bailey 2005; Di Sisto & Brunini 2007; Brassier et al. 2012b; Nesvorný et al. 2017; Fernández, Helal & Gallardo 2018; Kaib et al. 2019). By propagating the evolution of the early flat planetesimal disc 4.6 Gyr in the future, all surviving objects, including Centaurs, share the same age with the Solar system.

¹In time-backward integrations, collisions are unphysical. Time-backward ejection means time-forward capture.

* E-mail: namouni@oca.eu (FN); helena.morais@rc.unesp.br (MHMM)

So are the Centaurs' real past lifetimes short or can they be as long as the Solar system's age? This question may be answered if the literal interpretation of the dynamical lifetime is applied consistently to both past and future. This interpretation would therefore require the Centaur to reach the Solar system from the interstellar medium around say 10 Myr in the recent past only to leave the Solar system 10 Myr in the near future as the past and future lifetimes are similar. This would imply that the Solar system happens to be crossing the Centaur's path in the Galaxy around the current epoch and that its capture process from the interstellar medium should be fine-tuned to yield a stay of 20 Myr centred on our current epoch. Making our current epoch a privileged time in the Solar system's history to observe each known Centaur in the middle of its short Solar system stay violates the Copernican principle. Therefore, the past lifetime cannot be an indication of the actual age of a real Centaur and the physical instability of its orbit. It is probably a measure of the chaotic nature of motion at a Centaur's location. Consequently, the Centaur's age can be arbitrarily large. Planetesimal disc relaxation models are therefore justified in assuming that Centaurs may have the age of the Solar system regardless of their short past dynamical lifetimes.

To understand why no real² Centaur orbit was known to be stable over the age of the Solar system, it is necessary to know precisely how the dynamical evolution of real Centaurs is studied. We will only speak of Centaurs that were observed at multiple oppositions as their orbits are known with a reasonable degree of certainty. In order to assess the stability of a real Centaur's orbit, a clone swarm is replicated from its nominal orbit consistent with the observational error bars, and their equations of motion are integrated numerically. The future and past dynamical lifetimes correspond to the median clone survival time in the future and in the past, respectively. Two parameters enter the evolution simulation: the integration timespan and the clone number. The first is usually shorter than the age of the Solar system because the median lifetime inferred from the first trials itself is short. The clone number usually ranges from 10^2 to 10^3 owing to the computational cost of integrating larger sets but also to the acquired idea that real Centaur orbits are unstable. However, as the orbital element space of a Centaur's orbit is six-dimensional (3 positions and 3 velocities), clone sets of 10^2 and 10^3 correspond, respectively, to grids of approximately 2 points and 3 points within the error bar of each orbital element. These resolutions are insufficient to probe the Centaurs' stable orbits as they reside in one of the most chaotic regions of the Solar system.³ As a result, the dynamical integration of real Centaurs' motion in past studies is systematically unstable and remains in contradiction with the theoretical stable Centaur orbits found in disc relaxation models.

Progress was recently achieved in the study of Centaur origin in the outer Solar system with the development a high-resolution statistical search for stable orbits that led to the identification of the interstellar origin of Jupiter's retrograde co-orbital asteroid (514107) Ka'epaoka'awela (Namouni & Morais (2018b; hereafter Paper I). A swarm of a million clones was integrated backward in time for 4.5 Gyr to the epoch when planet formation ended. About half the number of clones collided with the Sun whereas the other

half was ejected from the Solar system. The median clone lifetime was 6 Myr. Of the million clone swarm, 46 members survived the age of the Solar system demonstrating that a real Centaur can be as old as the Solar system thus satisfying the Copernican principle and proving for the first time that the past dynamical lifetime is an indication of the strength of non-linearity in the neighbourhood of a Centaur's orbit. The 46 stable clones may constitute a small set with respect to the original million. However, the million sample is equivalent to a grid of just 10 points within the error bar of each orbital parameter. The low stable orbit rate therefore reflects the intrinsic limited resolution in each orbital parameter. It should also be noted that the existence of Centaur stable orbits over the age of the Solar system does not preclude a possible interstellar origin as is shown by asteroid Ka'epaoka'awela's example.

The high-resolution statistical orbit search applied to specific real objects is new and was used for the first time in the study of asteroid Ka'epaoka'awela. It is not a model of Centaur origin but a precise orbit determination method that it is not based on ad hoc initial conditions such as the primordial planetesimal disc's attributes that are used in typical relaxation models in the literature (Levison & Duncan 1997; Tiscareno & Malhotra 2003; Emel'yanenko et al. 2005; Di Sisto & Brunini 2007; Brasser et al. 2012b; Nesvorný et al. 2017; Fernández et al. 2018; Kaib et al. 2019). Provided the number of clones is sufficiently large, the method has, in effect, no parameter that can be modified to fine-tune its outcome. The method inputs the real asteroid's nominal orbit and the covariance matrix that represents the observational uncertainty and yields a probability distribution of the possible orbits that the asteroid had at the end of planet formation. The method may therefore be used on real objects to test planetesimal disc relaxation models and the ad hoc assumptions they make about the initial state of the Solar system.

In this work, we study the possible origins of high-inclination Centaurs and independently test whether they originate from the flat planetesimal disc of the conventional theory of Solar system formation (Pfalzner et al. 2015). We apply the high-resolution statistical orbit search to multiple-opposition high-inclination Centaurs and the two trans-neptunian objects (TNOs) with polar orbits. We call high-inclination Centaurs those with orbital inclinations from 60° to 180° encompassing prograde, polar, and retrograde motion. We limit our study to high inclinations for three reasons: first, previous work has shown that resonance capture, an essential dynamical process for all Centaurs, is more efficient for nearly polar and retrograde motion than for prograde motion thereby extending high-inclination Centaur lifetimes in the Solar system (Namouni & Morais 2015, 2017; Morais & Namouni 2017).

Secondly, if high-inclination Centaurs originate in the flat planetesimal disc, most of their clones will have low inclinations allowing us to confirm their evolution within the conventional view of Solar system formation. If however such objects retain high inclinations over the age of the Solar system, then the interstellar medium is a more probable origin. It is generally believed that when planet formation ended 4.5 Gyr in the past, the planets and the remaining compact and thin planetesimal disc that extended no further than Neptune's current orbit (Gomes, Morbidelli & Levison 2004), were nearly co-planar in order to explain the low-inclination reservoirs such as the asteroid and Kuiper belts through the gravitational relaxation of the system formed by the disc and the planets (Pfalzner et al. 2015).

Thirdly, the high-resolution statistical search applied to 20 asteroids requires about 2×10^7 clones implying a significant computational volume. For comparison, however, we also simulated the evolution of (2060) Chiron, a low inclination Centaur, that helps

²As opposed to the theoretical objects that represent Centaurs in planetesimal disc relaxation models whose orbits are stable over 4.6 Gyr.

³In mathematical terms, low resolution searches cannot identify the sticky tori of the dynamical system known to persist in the chaotic sea even in the case of high non-linearity (Zaslavsky 2007).

us illustrate the dependence of the stable orbit rate on the orbit's uncertainty level.

The paper is organized as follows. In Section 2, we present the Centaur and TNO sample and describe the simulation's setting. In Section 3, we discuss the statistics of stable and unstable motion and show that 4.5 Gyr-stable orbits exist for all objects in the study and originate in the scattered disc and inner Oort cloud regions. In Section 4, we discuss the Centaurs' interstellar origin and the possible dynamical identification of common capture events from the interstellar medium in the early Solar system.

2 OBJECT SAMPLE AND SIMULATION METHOD

The IAU Minor Planet Center⁴ lists 17 multiple-opposition Centaurs with inclinations larger than 60° and perihelia larger than 3 au as of 2018 December 1. The perihelion criterion is to limit the effect of the inner planets on the Centaurs' evolution. For convenience, Centaurs are divided into three groups. The first is the polar Centaurs group whose orbital planes are located within 30° from the direction of the Solar system's total angular momentum. In order of increasing inclination, this group includes 2010 FH92, 2007 BP102, 2010 CR140, (144908) 2004 YH32, (518151) 2016 FH13, 2014 JJ57, 2011 MM4, (342842) 2008 YB3, and 2016 LS. The second group is that of retrograde Centaurs that were studied in Morais & Namouni (2013b) to show that Jupiter and Saturn temporarily capture Centaurs in retrograde mean motion resonance. The objects are 2009 QY6, 1999 LE31, 2006 BZ8, (330759) 2008 SO218, and (434620) 2005 VD.⁵ The third group is that of Centaurs located in or near a planet's co-orbital region; it includes 2015 YY18 in Uranus' co-orbital region, and the two objects 2005 NP82 and 2016 YB13 near or in Jupiter's coorbital region to which Ka'epaoka'awela, Jupiter's coorbital asteroid, is added for comparison. The polar Centaur 2010 CR140 that is also located near Jupiter's coorbital region was not included in the co-orbital group because the capture probability in Jupiter's coorbital region for nearly polar orbits is small (Namouni & Morais 2018a).

To the high-inclination Centaurs, we add a fourth group with the two known polar TNOs 2008 KV42 and (471325) 2011 KT19, and a fifth with the low-inclination Centaur (2060) Chiron. The distribution of the sample objects in the xz -plane ($y = 0$) in terms of their semimajor axes, inclinations, perihelion, and aphelion distances is shown in Fig. 1. The first three columns of Table 1 list, respectively, the inclination I , eccentricity e , semimajor axis a , and perihelion distance q .

The Centaur and TNO nominal orbits and their equinoctial covariance matrices were obtained from the AstDys database⁶ for the Julian date 2458200.5 for all objects except 2005 NP82, 2010 CR140, and Chiron for which 2458400.5 was used (the Julian date 2457800.5 was used for Ka'epaoka'awela in Paper I.) The planets' orbital elements were obtained from NASA JPL's Horizons ephemeris system⁷ for the same epochs. To apply our high-resolution statistical search for stable orbits, clones were generated for each object as in Paper I using the Cholesky method

⁴<http://www.minorplanetcenter.net>

⁵Although 2009 QY6 and 2006 BZ8 have perihelia near 2 au, they were included in the study as they had demonstrated retrograde resonance capture with Jupiter and Saturn in our earlier work.

⁶<http://hamilton.dm.unipi.it/astdys> (Knežević & Milani 2012).

⁷<http://ssd.jpl.nasa.gov> (Giorgini et al. 1996).

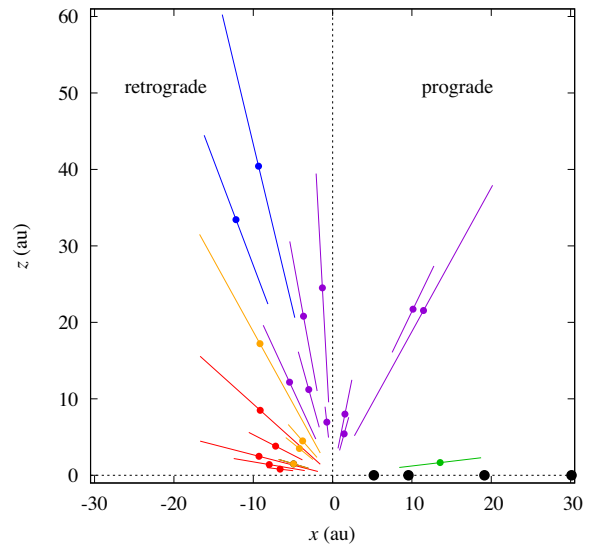


Figure 1. Distribution of the Centaur and TNO sample. Each segment represents the aphelion and perihelion excursions centred around the object's semimajor axis (filled circle) and is inclined with respect to the planets' reference plane. The polar Centaurs are purple, TNOs are blue, coorbital objects are orange, retrograde Centaurs are red, (2060) Chiron is green, and the four giant planets are black.

for multivariate normal distributions in order to best reproduce the uncertainty amplitudes of their orbits (Thomopoulos 2013).

In order to characterize the spread of a clone swarm in parameter space (or equivalently an orbit's uncertainty), we make use of the generalized variance of the equinoctial covariance matrix C (Wilks 1932). The latter is defined as the determinant of the covariance matrix $\det C$ and is used to estimate with a single number the spread of multidimensional samples. As we seek to compare the swarm spreads of different objects to ascertain how the stable clone rate depends on the orbit's uncertainty, we define the relative generalized deviation of the orbit $\text{RGD} = [\det C / (\prod_{1 \leq i \leq 6} e_i^2)]^{1/12}$ where e_i are the six nominal equinoctial orbital elements. The generalized variance is divided by the product of all the orbital elements squared in order to obtain relative and not absolute spread estimates. The twelfth root is used to make the generalized deviation of the same order as a standard deviation since the covariance matrix elements are proportional to the square of standard deviation and C is six-dimensional. The RGDs of the Centaur and TNO orbits are listed in the fourth column of Table 1.

The evolution of a Centaur clone back in time to -4.5 Gyr when planet formation ended, was followed in the system composed of the four giant planets and the Sun whose mass was augmented by those of the inner Solar system's planets. The full three-dimensional Galactic tide (Heisler & Tremaine 1986) and relative inclination of the ecliptic and Galactic planes were taken into account. The Oort constants ($A = 15.3$, $B = 11.9 \text{ km s}^{-1} \text{ kpc}^{-1}$) and star density in the Solar neighbourhood ($\rho_0 = 0.119 M_\odot \text{ pc}^{-3}$) are those derived from Gaia's first data release (Bovy 2017; Widmark & Monari 2019). Numerical integration of the five-body problem was carried out using the Bulirsch and Stoer algorithm with an error tolerance of 10^{-11} as in Paper I. Orbital evolution was monitored for collisions with the Sun, collisions with the planets, ejection from the Solar system, and reaching the inner 1 au semimajor axis boundary. No event at the inner boundary was registered for any of the Centaurs or TNOs.

Table 1. Clone statistics at -4.5 Gyr. Orbital inclination is denoted by I , eccentricity by e , semimajor axis by a , and perihelion by q . RGD stands for the relative generalized deviation of the Centaur's orbit. T_0 and T_m are the minimum and median lifetimes. Orbital elements are not given to nominal orbit precision to avoid an overcrowded table.

Asteroid	I ($^\circ$)	e	a (au)	q (au)	RGD (10^{-6})	Sample (10^6)	T_0 (10^4 yr)	T_m (10^6 yr)	Stable orbits	Sun collisions	Ejections	Planet collisions
Polar Centaurs												
2010 FH92	62	0.76	24.41	5.78	0.58	1	3.09	2.19	15	242 076	757 843	66
2007 BP102	65	0.26	23.98	17.75	2.30	0.12	2.73	29.84	219	24 151	95 612	18
2010 CR140	75	0.40	5.62	3.33	0.64	2	0.24	0.46	14	894 157	1105 395	434
(144908) 2004 YH32	79	0.56	8.16	3.55	0.24	2	0.78	0.68	17	873 118	1126 566	299
(518151) 2016 FH13	93	0.61	24.55	9.46	0.29	0.3	5.09	14.66	361	70 951	228 650	38
2014 JJ57	96	0.29	6.99	4.94	1.11	1	0.12	0.83	24	435 377	564 313	286
2011 MM4	100	0.47	21.13	11.14	3.22	0.3	1.47	31.39	1295	69 860	228 776	69
(342842) 2008 YB3	105	0.44	11.62	6.50	0.25	1	4.46	2.69	129	299 924	699 699	248
2016 LS	114	0.61	13.34	5.23	1.42	1	0.94	2.43	106	254 791	744 858	245
Retrograde Centaurs												
2009 QY6	137	0.83	12.47	2.06	0.37	1	3.80	3.26	41	446 095	553 637	227
1999 LE31	152	0.47	8.13	4.34	1.32	1	0.60	2.62	69	301 341	698 136	454
2006 BZ8	165	0.80	9.60	1.89	0.36	1	0.15	2.11	37	389 485	610 127	351
(330759) 2008 SO218	170	0.56	8.11	3.53	0.32	1	0.41	2.56	95	277 445	721 968	492
(434620) 2005 VD	173	0.25	6.67	4.99	1.65	1	0.08	2.41	91	275 162	724 175	572
Uranus coorbital												
2015 YY18	118	0.83	19.50	3.29	0.27	1	1.58	2.17	28	375 417	624 418	137
Jupiter coorbitals												
2005 NP82	130	0.48	5.87	3.06	0.21	1	0.11	1.33	17	487 264	512 286	433
2016 YB13	140	0.41	5.46	3.23	0.45	1	0.64	1.64	31	443 919	555 453	597
(514107) Ka'epaoka'awela	163	0.38	5.14	3.18	0.45	1	29.11	6.48	46	553 811	445 678	465
Polar TNOs												
2008 KV42	103	0.49	41.50	21.10	6.91	0.12	211.29	811	9504	18 585	91 885	26
(471325) 2011 KT19	110	0.33	35.58	23.81	0.64	0.12	139.35	511	9359	20 567	90 041	33
Prograde Centaur												
(2060) Chiron	7	0.38	13.66	8.45	0.05	1	0.26	1.09	303	106 731	891 886	1080

The clone number for each object was chosen with respect to the clone median lifetime determined from the first 10^4 clone simulation. For a lifetime in excess of 10^7 yr, the number of 4.5 Gyr-stable clones is relatively large and the statistics is determined with smaller clone sets in order to reduce computational volume. The clone number varies from 1.2×10^5 for 2007 BP102, 2008 KV42, and 2011 KT19 to 3×10^5 for 2016 FH13 and 2011 MM4. For smaller lifetimes and most objects, 10^6 clones are used as in Paper I unless the stable clone rate is $< 10^{-5}$, then the clone number is increased to 2×10^6 (2010 CR40 and 2004 YH32).

In the selected object sample, only Centaur (2060) Chiron is known to have exhibited cometary activity. Whereas the effect of non-gravitational forces is important in a comet's evolution, we do not include such processes in this study. Cometary activity is a complex phenomenon whose simplified modelling in the context of comet dynamics may produce less agreement with observations than a conservative approach (Wiegert & Tremaine 1999). As gravitational systems tend to the stable states available to them, the conservative simulation of Chiron's motion offers information on the stability of its current orbit and helps illustrate how the 4.5 Gyr-stable orbit rate depends on the orbit's uncertainty.

3 STATISTICS

The dynamical lifetimes and the clone statistics at -4.5 Gyr are given in Table 1. Regardless of orbit uncertainty (RGD), the Centaur minimum lifetime scales as 10^3 – 10^4 yr except those of Ka'epaoka'awela and the two TNOs which are ~ 1 Myr because

of their privileged locations in the Solar system's strongest mean motion resonance for the first one and beyond Neptune's orbit for the latter two. The high-inclination Centaur median lifetime T_m ranges from 1 to 30 Myr, and is consistent with that of Centaurs generally (Tiscareno & Malhotra 2003; Horner et al. 2004). TNOs have longer median lifetimes of 0.5 Gyr for 2001 KT19 (Chen et al. 2016) and 0.8 Gyr for 2008 KV42. Surprisingly, 8 out of the 17 high-inclination Centaurs have median lifetimes that cluster around 2.4 Myr with a standard deviation of 0.2 Myr. They are 2015 YY18, 1999 LE31, 2006 BZ8, 2008 SO218, 2005 VD, 2010 FH92, 2008 YB3, and 2016 LS. We discuss in Section 4, the possibility of mapping phase space using the median lifetime to ascertain whether the 2.4 Myr-lifetime Centaurs followed the same path in their evolution from the outer Solar system and were initially captured in similar conditions. The longest Centaur median lifetimes are found in the polar group with 15 Myr for 2016 FH13 and 30 Myr for both 2007 BP102 and 2011 MM4. Long median lifetimes seem to be correlated with large perihelia. We searched for correlations between the ratio of the minimum and median lifetimes and the RGD without success as we sought to ascertain whether the minimum lifetime scaled to the median lifetime is an indicator of the level of orbit uncertainty.

Clone instability is mainly achieved by ejection and Sun collisions. Planet collisions are rare. Like the median lifetime, the relative statistics of unstable orbits show definite trends regardless of orbit uncertainty. Except for Ka'epaoka'awela, the fraction of ejected clones is always larger than that of Sun-colliding clones. Jupiter acts as a strong protector for Ka'epaoka'awela through its

co-orbital resonance and as a strong perturber for all other Centaurs. In the polar group, the ejection rate increases with semimajor axis from ~ 55 per cent to 80 per cent and the Sun-collision rate decreases accordingly with the sum of the two rates $\lesssim 100$ per cent. The opposite trend occurs in the retrograde group. The 2.4 Myr-median lifetime group have ejection and Solar collision rates clustered around 70 per cent and 30 per cent, respectively, with a standard deviation of 5 per cent for both rates.

TNO clones are unstable largely through ejection at 75 per cent and through Solar collisions at 17 per cent whereas the largest rate of orbit ejection is by far Chiron's at 90 per cent as the orbit's low inclination maximizes the likelihood of disruption by close encounters with the planets.

Orbits that survive the age of the Solar system exist for all objects in the study: high-inclination Centaurs, the two TNOs as well as Chiron. The fraction of stable clones of high-inclination Centaurs ranges from 0.0007 per cent (2010 CR140) to 0.43 per cent (2011 MM4). In the 2.4 Myr lifetime-group, the stable orbit rate is on average 0.007 per cent with a standard deviation of 0.004 per cent. The two TNOs have by far the largest stable orbit rate of 8 per cent whereas Chiron stands at 0.03 per cent.

Large fractions of stable clones are naturally correlated with long median lifetimes. They are also related to the orbit's uncertainty. The most salient example is Chiron whose orbit is inclined by 7° with respect to the planets and is located in a largely chaotic region as indicated by its 1 Myr-median lifetime and its high planet collision rate. However, with 49 oppositions, it is by far the most observed object in the study. Consequently, its orbit has the smallest RGD $= 5 \times 10^{-8}$ one to two order of magnitude smaller than the other objects in the study. This reflects on its stable orbit rate that is by far the highest among Centaurs with similar median lifetimes. The two TNOs have RGDs that differ by an order of magnitude but the median lifetime of the more uncertain orbit (2008 KV42) is about twice that of the less uncertain one (2011 KT19). The similar stable orbit rates of the two TNOs suggest that the long median lifetime of 2008 KV42, that signifies a less chaotic neighbourhood than 2011 KT19's, compensates its larger observational uncertainty than that of (2011) KT19. In the 2.4 Myr group, there is no clear relationship between RGD and stable orbit rate.

The distribution of stable clones at -4.5 Gyr is shown in Fig. 2 in terms of their eccentricity e , inclination I , and semi-major axis a along with the current position of the object's orbit. For convenience, we divide the stable clones locations into six groups: the inner Solar system with $4 \leq a(\text{au}) < 5.2$, planet coorbitals, the Centaur region $5.2 < a(\text{au}) < 30$, the Kuiper belt region $30 \leq a(\text{au}) \leq 50$, the scattered disc region $50 < a(\text{au}) \leq 10^3$, and the Oort cloud region $a(\text{au}) > 10^3$. The 10^3 au frontier delineates the region beyond which the Galactic tide's effects are important (Fig. 2). The breakdown of the stable clones' location is given for all objects in Table 2. Except for Ka'epaoka'awela, the vast majority of stable clones are found in the scattered disc and Oort cloud regions. Clones in the co-orbital state, the inner Solar system, the Centaur region and the Kuiper belt region are rare. The latter are present mainly for objects with large stable orbit rates such as those with large median lifetimes and Chiron whose orbit uncertainty level is low. Below a current inclination of 80° , the polar Centaurs' clones tend to be equally divided between the scattered disc and Oort cloud regions with a preference for the latter (2007 BP102). Above the threshold inclination, there is a clear preference of all objects for the scattered disc, including the two TNOs and Chiron whose clone ratio for the two regions is 2.

For objects with large stable orbit rates, the probability density and the empirical cumulative distribution function at -4.5 Gyr can

show additional features regarding the distribution of the orbital elements. These functions are shown for 2016 FH13, 2011 MM4, 2008 KV 42, and Chiron in Fig. 3. The semimajor axis, eccentricity, and inclination probability densities were binned in 10 au, 0.01, and 1° intervals, respectively. The semimajor axis distributions of the four objects peak between 70 and 100 au with a smaller secondary peak in the inner Oort cloud. Probability density peaks show as inflection points on the (unbinned) cumulative distribution function. The inclination probability densities have a single peak between 70° and 90° except for Chiron whose mean inclination is 29° . The eccentricity probability densities peak between 0.8 and 0.9 and reflect for all objects the path followed by the clones. With perihelia near the orbits of the planets, clone eccentricity is invariably raised by planetary close encounters. If the clone reaches the Oort cloud region, the Galactic tide lowers its eccentricity and increases its inclination in a secular periodic cycle (Heisler & Tremaine 1986).

The stable orbits found in the scattered disc and Oort cloud regions all have high inclinations and are shown in Fig. 4 in terms of their mean values and standard deviations for all objects as functions of the object's current inclination. Excluding Chiron, the only low-inclination Centaur, the mean inclination at -4.5 Gyr in the scattered disc region is an increasing function of the inclination at the current epoch. It starts at $\sim 55^\circ$ for a current inclination of $\sim 60^\circ$ and reaches asymptotically to 90° as current inclination increases to 180° . Standard deviation is approximately 10° . In the Oort cloud region a similar trend is found albeit with larger mean inclination scatter and larger standard deviations explained naturally by the effect of the Galactic tide as can be seen in Fig. 2. The parameter space structure containing the nearly polar orbits was termed as the polar corridor in Paper I and identified as the most favourable location for Centaurs that were captured by Jupiter and moved away from its orbit.

Chiron's mean inclinations and standard deviations in the scattered disc and Oort cloud regions at -4.5 Gyr, respectively, are $28^\circ \pm 11^\circ$ and $33^\circ \pm 14^\circ$. For all objects, the stable clones found in the scattered disc region have perihelia near Uranus's and Neptune's orbit (Fig. 2). In effect, as expected for Centaur-type motion, clones are scattered by the four giant planets towards the inner and outer parts of the Solar system. Those sent towards the inner Solar system are largely unstable as they are subjected to the perturbing effect of Jupiter and Saturn. Stable clones that are scattered to the outer Solar system are ultimately locked to Uranus's or Neptune's perihelia unless they reach the Oort cloud region where the Galactic tide lowers their eccentricity and inclinations periodically. The stable clones found in the Oort cloud region share the same domain with a semimajor axis centred around 2800 au of width 1200 au (standard deviation; Fig. 4). This domain corresponds to the secondary peaks of the semimajor axis distributions shown in Fig. 3.

4 DISCUSSION

In this work, we have applied a precise orbit determination method to determine the possible orbits of real high-inclination Centaurs and TNOs at the end of planet formation. The statistical nature of this method implies that only probability distributions can be derived regarding the early orbits of the studied asteroids. This characterization is sufficient to point out the origin of the studied objects. It enabled us for instance to show that all high-inclination Centaurs in the study had probably nearly polar inclinations 4.5 Gyr in the past. If high-inclination Centaurs had originated from the flat planetesimal disc of standard Solar system formation theory, our statistical method would have found a majority of clones with

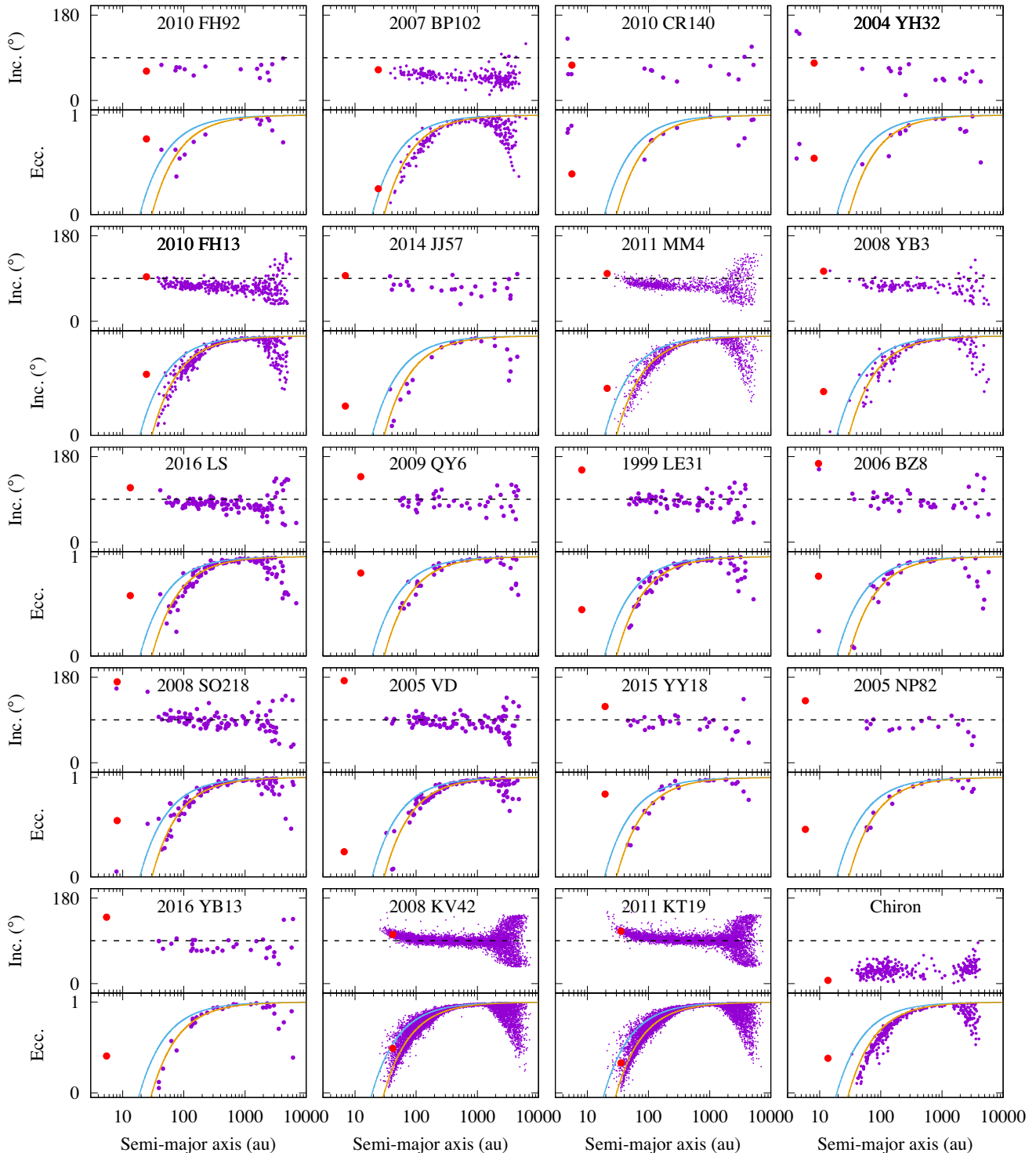


Figure 2. Distribution of stable orbits in the eccentricity-semimajor axis and inclination-semimajor axis planes at -4.5 Gyr. The location of the object at the current epoch is indicated with a large red filled circle. The locus of intersection of the objects' perihelion with Uranus's and Neptune's orbits are shown with the top blue curve and the bottom orange curve, respectively.

relatively small inclinations near the common orbital plane of the outer planets for each of the objects in the study.

Provided that the clone number is sufficiently large, our orbit determination method does not depend on any ad hoc initial conditions such as those inherent to planetesimal disc relaxation models that research the origin of outer Solar system objects. In this

respect, the method is not a model and its derived statistical orbit distributions for high-inclination Centaurs are robust and may not be fine-tuned to change the outcome of the simulation. The probability distributions can only be improved by further observations that reduce the uncertainty level of the studied objects' orbits. That is why this method can independently test origin theories of outer

Table 2. Clone location breakdown at -4.5 Gyr. ISS indicates the inner Solar system ($4 \leq a(\text{au}) < 5.2$), 1:1 the coorbital resonance, CEN centaurs ($5.2 < a(\text{au}) < 30$), KB the Kuiper belt ($30 \leq a(\text{au}) \leq 50$), SD the scattered disc ($50 < a(\text{au}) \leq 10^3$), and OC the Oort cloud ($a(\text{au}) > 10^3$). For the 1:1 resonance, the planet's initial identifies the asteroid's location.

Asteroid	ISS	1:1	CEN	KB	SD	OC
Polar Centaurs						
2010 FH92	0	0	0	1	7	7
2007 BP102	0	0	0	3	92	124
2010 CR140	1	2J	0	0	5	6
(144908) 2004 YH32	2	0	0	1	7	7
(518151) 2016 FH13	0	0	0	12	203	146
2014 JJ57	0	0	0	3	13	8
2011 MM4	0	1N	2	32	750	510
(342842) 2008 YB3	0	1N	1	1	80	46
2016 LS	0	0	0	1	66	39
Retrograde Centaurs						
2009 QY6	0	0	0	0	24	17
1999 LE31	0	0	0	1	46	22
2006 BZ8	0	1S	0	2	23	11
(330759) 2008 SO218	0	0	2	3	58	32
(434620) 2005 VD	0	0	0	4	50	37
Uranus coorbital						
2015 YY18	0	0	0	1	19	8
Jupiter coorbitals						
2005 NP82	0	0	0	0	11	6
2016 YB13	0	0	0	3	16	12
(514107) Ka'epaoka'awela	0	27J	0	0	10	9
Polar TNOs						
2008 KV42	0	3N	6	287	6255	2953
(471325) 2011 KT19	0	8N	16	314	6256	2765
Prograde Centaur						
(2060) Chiron	0	0	0	15	193	95

Solar system's objects by following back in time the motion of real Solar system objects.

To interpret precisely the finding that high-inclination Centaurs had nearly polar orbits at the end of planet formation, it is useful to recall the current understanding of early Solar system structure (Pfalzner et al. 2015). The Solar system started forming 4.6 Gyr in the past. Sometime after a few Myr, giant planets formed and radially migrated while interacting with the planetesimal disc. The migration relaxation time is thought to have been about 1 to a few 10 Myr whereas the full migration stage is thought to have lasted about a 100–500 Myr at the end of which the planets reached their final orbits. The planets' orbital evolution in this stage is largely uncertain owing to the multitude of complex processes that operate in the first 100 Myr of planet formation (Ribeiro et al. 2020). What is certain, however, is first, that the planetesimal disc before the migration stage as well as at the end of this stage had a small inclination dispersion in order to explain the very low inclination TNOs currently observed in the Kuiper belt (known as the cold population) (Pfalzner et al. 2015). Secondly, the early planetesimal disc could not have extended beyond 30–40 au (Gomes et al. 2004) to ensure that Neptune does not end up with a much larger final semimajor axis than the current one. Thus the early scattered disc and Oort cloud were devoid of Solar system material. Our orbit determination method was run for 4.5 Gyr in the past. The fact that the planets migrated towards the end of that period is not included in our calculation because the planets' evolution in the migration stage

is largely uncertain but more importantly, because it does not affect the Centaur orbits end states in any significant way. The reason lies in the fact that the bulk of stable Centaur clones that end up on nearly polar orbits do so in the first 1 Gyr of the simulation. Therefore near 4 Gyr in the past, the polar stable clones are already located far away in the scattered disc and the inner Oort cloud. Changes in the planets' semimajor axes over a few 10 Myr do not affect such distant polar orbits significantly, as in reality, the planets' effect had long started to decay in the last billion years before migration even occurred.

The high likelihood of nearly polar 4.5 Gyr-stable orbits for high inclinations Centaurs in regions devoid of Solar system material indicates that they did not belong to the nearly flat early planetesimal disc and have probably been captured from the interstellar medium. The Sun's birth cluster of stars naturally provided a significant source of asteroids and comets for the Sun and the planets to capture during an epoch where gas in the Solar system and the interstellar medium was present to help seal temporarily trapped objects into permanent orbits around the Sun (Fernández & Brunini 2000; Levison et al. 2010; Brassier et al. 2012a; Jílková et al. 2016; Hands et al. 2019).

Centaur capture from the interstellar medium has been invoked in a recent work (Kaib et al. 2019) that examined disc relaxation models against the observed population of Centaurs and TNOs in the outer Solar system survey (OSSOS). Whereas that sample included only one high-inclination TNO (2008) KV42, present in our study, and mainly low-to-moderate inclination orbits ($\leq 53^\circ$ with a median of 14°), the authors concluded that reproducing the high inclinations observed in their sample is not explained by the relaxation of the planetesimal disc with or without an additional hypothetical outer planet and that enrichment from the interstellar medium could solve this problem. Our findings confirm that conclusion. Interestingly, another recent work on calibrating the OSSOS Centaur detections concluded that classical planetesimal disc models do not explain the abundance of high-inclination Centaurs and that 'other sources may be needed' (Nesvorný et al. 2019).

Our finding that the probable origin of high-inclination Centaurs is the interstellar medium disagrees with earlier theories about Centaur origin being the relaxed primordial planetesimal disc (Levison & Duncan 1997; Tiscareno & Malhotra 2003; Emel'yanenko et al. 2005; Di Sisto & Brunini 2007; Brassier et al. 2012b). Since our approach relies on a precise orbit determination method for real Centaurs that does not invoke any ad hoc initial conditions, our obtained orbit probability distributions are robust. The question is then what is the difference between the objects seen in relaxation models (with ad hoc initial conditions) and identified as possible Centaurs, and the Centaur clones in this study? The main difference is related to the dynamical pathways followed by the two types of objects: the theoretical Centaurs and the real Centaurs in our work. Disc relaxation models do not have sufficient dynamical resolution to reproduce the dynamics of real objects. Instead the primordial planetesimal disc is spread over a large spatial extent and integrated forward in time from the end of planet formation to the current epoch. There is no certainty that the identified dynamical pathways in such simulations are those of real Solar system objects beyond the global comparisons in parameter space (orbital elements, perihelia, and Tisserand parameter) with entire populations of small bodies.

When 4.5 Gyr-stable orbits were found in Paper I for Ka'epaoka'awela with a majority of retrograde orbits in Jupiter's co-orbital region, it was concluded that Ka'epaoka'awela is likely of interstellar origin as no internal Solar system dynamical process could produce asteroid orbits with an inclination of 162° at

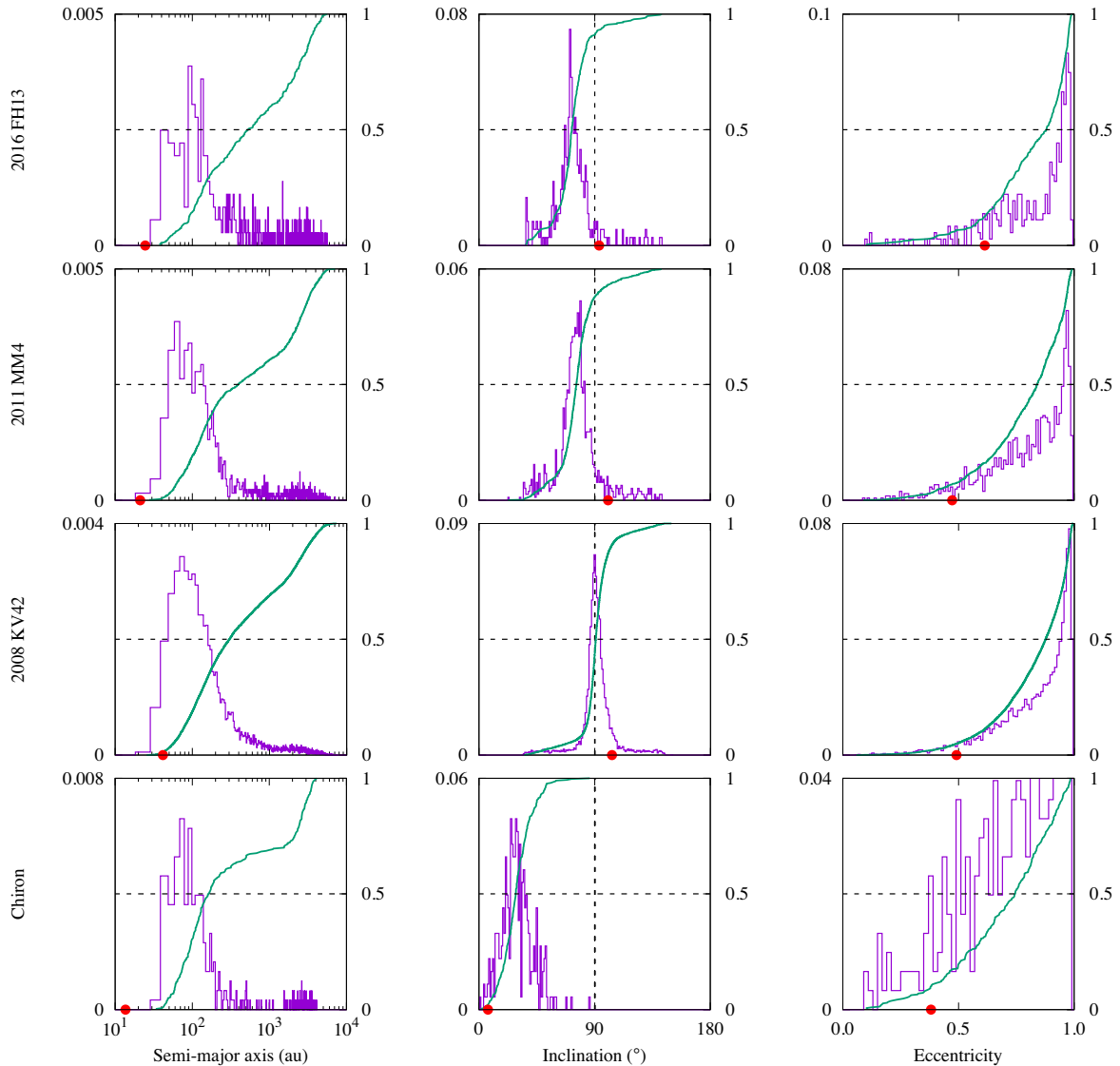


Figure 3. Probability densities (purple curves, left scales) and empirical cumulative distribution functions (green curves, right scales) of some high stable orbit rate objects at -4.5 Gyr. The red filled circle on the horizontal axis of each panel indicates nominal value of the corresponding orbital element at the current epoch.

Jupiter’s location at that early epoch. Ka’epaoka’awela could be a representative of a class of asteroids captured from the interstellar medium by the Sun and Jupiter owing to the strength of Jupiter’s co-orbital resonance at large inclination that is responsible for shielding the asteroid from disruptive perturbations from the other planets (Morais & Namouni 2013a, 2016; Namouni & Morais 2018b).

The existence of 4.5 Gyr-stable orbits for high-inclination Centaurs, the two polar TNOs and Chiron widens the significance of that earlier finding in that stability over the age of the Solar system is possible even for Centaurs that are not protected by strong resonances. Furthermore, high inclination is not a prerequisite for Centaur stability over the age of the Solar system as Chiron’s example demonstrates.

The definite trends that were identified from the statistics of unstable and stable orbits and the various relationships including the minimum and median lifetimes have the potential of shedding new light on the dynamical structure of phase space that classical local chaos indicators cannot. For instance the determination of the

typical time-scale for diverging orbits, classically used to identify dynamical chaos, would have concluded accurately only that all objects in the study are located in strongly chaotic regions of phase space. To gain more information regarding the existence of stable orbits, statistical methods are necessary to ascertain precisely the possible pathways that Centaurs navigate on stable orbits in order to transfer from as far out as the inner Oort cloud to the giant planets’ domain. In this regard, the surprising finding that 8 out of 17 high-inclination Centaurs have the same median lifetime of 2.4 ± 0.2 Myr could be an indication of a common pathway in phase space that was followed by objects captured under similar conditions or even in a single interstellar capture event.

Directly identifying the locations of capture events depends on the stable orbit rate. As explained in the Section 1, the million clone sample when projected on a single orbital space dimension is equivalent to sampling over 10 points within the error bar of the corresponding orbital element. With such limited sampling, looking for common origins among different objects requires that either median

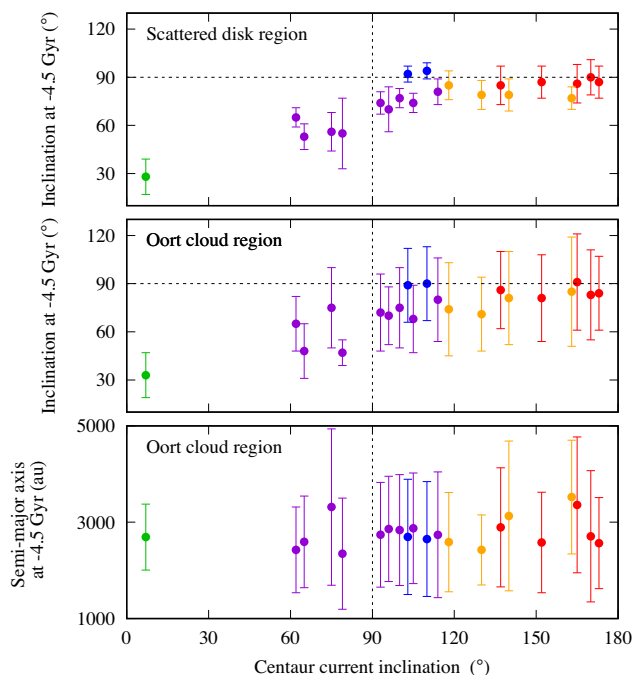


Figure 4. Scattered disk clone inclinations and Oort cloud clone inclinations and semimajor axes at -4.5 Gyr as functions of the Centaur’s inclination at the current epoch. The filled circles indicate the mean values, and the error bars the corresponding standard deviations. The colour codes are those of Fig. 1.

lifetime is large or that the orbit is known with great certainty. Both conditions guarantee a large stable orbit rate in order to favour clone clustering. An exception is given by Ka’ea’poka’awela’s location in Jupiter’s strongest resonance where a majority of clones cluster on a single orbit instead of being scattered across a wide expanse from 50 to 4000 au like all objects in this study. Identifying common origin is likely to succeed at low inclination as such Centaurs have the lowest uncertainty levels owing to their extended observation history. In this respect, one of the surprising findings of this study is the stability of Chiron. Although the simulation does not include non-gravitational forces, it shows that the current orbit is 4.5 Gyr-stable and had an initial mean inclination $\sim 30^\circ$. As the inclination dispersion of the planetesimal disc is believed to have been small before and after migration, there are two possibilities for its origin. Either Chiron is an outlier that belonged to the planetesimal disc and whose cometary activity by some unknown mechanism increased its inclination far above the planetesimal disc’s mid-plane, or it could be itself of interstellar origin. Asteroid capture in the Sun’s birth cluster does not necessarily favour objects whose orbits have or evolve to polar or high-inclination retrograde motion (Hands et al. 2019). An astronomical illustration of the principle may be found in the distribution of the irregular satellites of the giant planets. Applying the high-resolution statistical stable orbit search to low-inclination Centaurs is likely to shed light on the possible common capture events that occurred in the early Solar system.

ACKNOWLEDGEMENTS

We are grateful to the reviewers for their comments that helped improve the clarity of the paper. The orbital search simulations were done at the Mésocentre SIGAMM hosted at the Observatoire de la Côte d’Azur. MHM Morais research had financial support

from São Paulo Research Foundation (FAPESP/2018/08620-1) and CNPq-Brazil (Pq2/304037/2018-4). This research was supported in part by the Funding Authority for Studies and Projects of Brazil (FINEP) and the São Paulo Research Foundation (FAPESP) through the computational resources provided by the Center for Scientific Computing (NCC/GridUNESP) of the São Paulo State University (UNESP).

REFERENCES

- Bailey B. L., Malhotra R., 2009, *Icarus*, 203, 155
 Bovy J., 2017, *MNRAS*, 468, L63
 Brasser R., Duncan M. J., Levison H. F., Schwamb M. E., Brown M. E., 2012a, *Icarus*, 217, 1
 Brasser R., Schwamb M. E., Lykawka P. S., Gomes R. S., 2012b, *MNRAS*, 420, 3396
 Chen Y.-T. et al., 2016, *ApJ*, 827, L24
 Di Sisto R. P., Brunini A., 2007, *Icarus*, 190, 224
 Emel’yanenko V. V., Asher D. J., Bailey M. E., 2005, *MNRAS*, 361, 1345
 Fernández J. A., Brunini A., 2000, *Icarus*, 145, 580
 Fernández J. A., Helal M., Gallardo T., 2018, *Planet. Space Sci.*, 158, 6
 Giorgini J. D. et al., 1996, AAS/Division for Planetary Sciences Meeting Abstracts #28. p. 1158
 Gomes R. S., Morbidelli A., Levison H. F., 2004, *Icarus*, 170, 492
 Hands T. O., Dehnen W., Gration A., Stadel J., Moore B., 2019, *MNRAS*, 419, 1064
 Heisler J., Tremaine S., 1986, *Icarus*, 65, 13
 Horner J., Evans N. W., Bailey M. E., 2004, *MNRAS*, 354, 798
 Jílková L., Hamers A. S., Hammer M., Portegies Zwart S., 2016, *MNRAS*, 457, 4218
 Kaib N. A. et al., 2019, *AJ*, 158, 43
 Knežević Z., Milani A., 2012, IAU Joint Discussion, p. P18
 Levison H. F., Duncan M. J., 1997, *Icarus*, 127, 13
 Levison H. F., Duncan M. J., Brasser R., Kaufmann D. E., 2010, *Science*, 329, 187
 Morais M. H. M., Namouni F., 2013a, *Celest. Mech. Dyn. Astron.*, 117, 405
 Morais M. H. M., Namouni F., 2013b, *MNRAS*, 436, L30
 Morais M. H. M., Namouni F., 2016, *Celest. Mech. Dyn. Astron.*, 125, 91
 Morais M. H. M., Namouni F., 2017, *MNRAS*, 472, L1
 Namouni F., Morais M. H. M., 2015, *MNRAS*, 446, 1998
 Namouni F., Morais M. H. M., 2017, *MNRAS*, 467, 2673
 Namouni F., Morais M. H. M., 2018a, *J. Comp. App. Math.*, 37, 65
 Namouni F., Morais M. H. M., 2018b, *MNRAS*, 477, L117
 Nesvorný D., Vokrouhlický D., Dones L., Levison H. F., Kaib N., Morbidelli A., 2017, *ApJ*, 845, 27
 Nesvorný D. et al., 2019, *AJ*, 158, 132
 Peixinho N., Thirouin A., Tegler S. C., Di Sisto R. P., Delsanti A., Guilbert-Lepoutre A., Bauer J. G., 2020, Chapter in The transneptunian Solar system, Elsevier, Amsterdam, p. 307
 Pflanzner S. et al., 2015, *Phys. Scr.*, 90, 068001
 Portegies Zwart S. F., Boekholt T. C., 2018, *Commun. Nonlinear Sci. Numer. Simul.*, 61, 160
 Ribeiro R. d. S., Morbidelli A., Raymond S. N., Izidoro A., Gomes R., Vieira Neto E., 2020, *Icarus*, 339, 113605
 Thomopoulos N. T., 2013, Essentials of Monte Carlo Simulation. Springer-Verlag, New York
 Tiscareno M. S., Malhotra R., 2003, *AJ*, 126, 3122
 Volk K., Malhotra R., 2013, *Icarus*, 224, 66
 Widmark A., Monari G., 2019, *MNRAS*, 482, 262
 Wiegert P., Tremaine S., 1999, *Icarus*, 137, 84
 Wilks S. S., 1932, *Biometrika*, 34, 471
 Zaslavsky G. M., 2007, The Physics of Chaos in Hamiltonian Systems, World Scientific, Singapore

This paper has been typeset from a $\text{\TeX}/\text{\LaTeX}$ file prepared by the author.